Measuring nondipolar asymmetries of photoelectron angular distributions

P. S. Shaw
Optical Technology Division, National Institute of Standards and Technology, Gaithersburg, Maryland 20899

U. Arp
Quantum Metrology Division, National Institute of Standards and Technology, Gaithersburg, Maryland 20899

S. H. Southworth
Physics Division, Argonne National Laboratory, Argonne, Illinois 60439
(Received 7 December 1995)

In theories of photoelectron angular distributions at soft-x-ray energies from 1 to 10 keV, first-order corrections to the dipole approximation give rise to two nondipolar asymmetry parameters in addition to the well-known dipolar asymmetry parameter β. The nondipolar parameters characterize the forward-backward asymmetry with respect to the propagation vector of the photon beam. Experimentally, the measurement of the nondipolar effect has been hampered because of the complications resulting from the three-parameter angular distribution. In this paper, we suggest various experimental approaches to the measurement of the three asymmetry parameters using partially linearly polarized x rays, corresponding to measurements on synchrotron radiation beamlines. We describe methods to extract the asymmetry parameters using such approaches. [S1050-2947(96)07908-5]

PACS number(s): 32.80.Fb, 32.80.Hd

I. INTRODUCTION

Atomic photoelectron angular distributions have been extensively studied at lower photon energies in the vacuum ultraviolet (VUV) region, where the dipole approximation to the photoemission matrix element is usually considered to be a good description of the interaction [1–4]. In the dipole approximation, the angular distribution for linearly polarized light depends only on the angle between the photon polarization vector and the photoelectron momentum vector and is completely characterized by one asymmetry parameter β. However, at higher photon energies in the VUV and in the x-ray region, nondipolar interactions can modify photoelectron angular distributions, resulting in a forward-backward asymmetry with respect to the photon propagation vector [5–10].

In theories which treat the photon-atom interaction beyond the dipole approximation, a general expression for photoelectron angular distributions, with angles referenced to the photon beam direction, can be given as an expansion in spherical harmonics:

$$I(\theta,\phi)=\sum_{L,M} b_{LM}Y_{LM}(\theta,\phi), \tag{1}$$

where the coefficients b_{LM} contain the dynamical information and the dependence on the polarization state of the photon beam. Peshkin [5] has emphasized the use of the density-matrix description of the photon polarization state and of the multipole expansion of the photon plane wave to separate polarization effects from dynamics and to determine the symmetry properties of angular distribution patterns imposed by conservation of angular momentum and parity. Assuming randomly oriented target atoms, the angular symmetry properties of the photon-atom system are constrained by the symmetry properties of the photon beam. The L values in Eq. (1) are determined by the number and type of multipole components included in the calculation, but the M values are restricted to 0, ± 2 due to the unit spin, odd intrinsic parity, and transversality condition of photons.

In specific calculations, the number of terms included in Eq. (1) is usually limited by truncation of the multipole expansion. At low photon energies, it is common to include only the electric-dipole interaction. Consequently, only $L=0$ and 2 terms are retained in Eq. (1), and the angular distribution is characterized by a single asymmetry parameter β. At the high-energy extreme ($\approx$1 MeV), Scofield [9] has indicated that about 100 multipoles are needed in calculations, which would give a very complicated form to the angular distribution. In such a case, it would seem to be impractical to measure all of the asymmetry parameters; instead, the calculations could be tested by measuring photoelectron intensities at selected angles. However, in the photon energy region of $\approx$5–10 keV, recent calculations suggest that it may be sufficient to characterize angular distributions via first-order corrections to the dipole approximation, i.e., by including interference terms between electric-dipole transition amplitudes and amplitudes for electric-quadrupole and magnetic-dipole interactions [8–10]. Terms of $L=0$–3 of Eq. (1) are included in this approximation, giving rise to two ''nondipolar'' asymmetry parameters in addition to the ''dipolar'' asymmetry parameter β.

General insight into the form of angular distributions corrected to first order beyond the dipole approximation is given by the differential cross section for linearly polarized light derived by Bechler and Pratt [8]:

$$\frac{d\sigma}{d\Omega}=\frac{\sigma}{4\pi}\{1+\beta P_2(|\boldsymbol{\varepsilon}\cdot\hat{\mathbf{p}}|)+(\hat{\mathbf{p}}\cdot\hat{\mathbf{k}})[a+bP_2(|\boldsymbol{\varepsilon}\cdot\hat{\mathbf{p}}|)]\}, \tag{2}$$

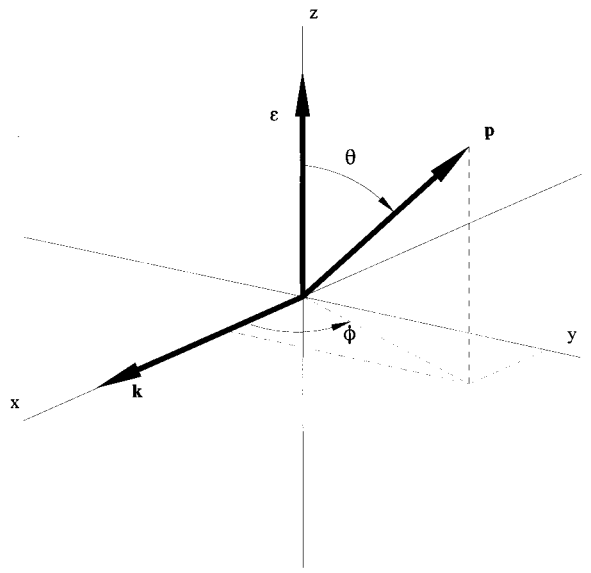

FIG. 1. The coordinate system used to describe the photoelectron angular distribution. Here, θ is the polar angle of the photoelectron momentum vector **p** with respect to the z axis (or the photon polarization vector $\boldsymbol{\varepsilon}$) and ϕ is the azimuthal angle defined by the projection of **p** in the x-y plane, which is perpendicular to $\boldsymbol{\varepsilon}$ and contains the photon propagation vector **k**.

where, as shown in Fig. 1, **p** is the photoelectron momentum vector, $\boldsymbol{\varepsilon}$ is the photon polarization vector taken along the z axis, **k** is the photon propagation vector taken along the x axis, β is the usual dipolar asymmetry parameter, and a and b are the nondipolar asymmetry parameters. In contrast with the dipole approximation, corresponding to $k\rightarrow 0$ in Eq. (2), the corrected cross section depends on the photoelectron emission angles relative to both **k** and $\boldsymbol{\varepsilon}$. The correction terms redistribute photoelectron intensity with respect to **k** and $\boldsymbol{\varepsilon}$, but do not contribute to the angle-integrated cross section σ calculated from the dipole amplitudes. The angular distribution no longer possesses rotational symmetry about the $\boldsymbol{\varepsilon}$ vector, as it has in the dipole approximation, but it retains reflection symmetry in the x-y and x-z planes. The correction terms vanish in the plane perpendicular to **k** (the y-z plane), so measurements made in this plane are sensitive only to the dipolar terms. Angle-resolved electron spectrometers designed to measure σ and β parameters by recording photoelectron intensities in the plane perpendicular to **k**, Ref. [11] for example, will be insensitive to nondipolar correction terms in energy regions where Eq. (2) is valid. However, other spectrometer systems designed for σ and β measurements, Refs. [12,13], for example, detect electrons emitted forward or backward with respect to **k** and will be sensitive to nondipolar terms in Eq. (2).

On the experimental side, in early measurements using unpolarized soft x rays, Krause and Wuilleùmier observed photoelectron angular distributions to be tilted in the forward direction with respect to the x-ray beam [14]. Only recently, an experiment using tunable synchrotron x rays was performed by Krässig *et al.*, who used 2- to 5-keV polarized x rays to measure forward-backward asymmetries for the Ar($1s$), Kr($2s$), and Kr($2p$) subshells [15]. In agreement with theoretical calculations [8–10], the measured asymmetries for different atomic subshells display different energy dependencies. At certain energies, Krässig *et al.* observed enhancement of the photoelectron intensity in the backward direction, while at other energies, the photoelectron intensity was enhanced in the forward direction. In analogy with studies of the β parameter at VUV energies [1–4], studies of nondipolar asymmetries provide additional insight into atomic photoionization at x-ray energies. With the advent of ''third-generation'' synchrotron light sources, we expect there will be increasing interest in measurements of nondipolar effects.

TABLE I. Relationships of the dipolar and nondipolar parameters, β, γ, δ, used by Cooper [10] and adopted by this paper, and the B_1, B_2, and B_3 of Scofield [9], the β, a, and b by Bechler and Pratt [8], and the β, κ, γ, and η by Amusia and Cherepkov [6]. Note that the equivalent table in Ref. [10] has an error in the relation between β and B_2.

Cooper [10]	Scofield [9]	Bechler and Pratt [8]	Amusia and Cherepkov [6]
β	$-2B_2$	β	β
γ	$-5B_3$	$3b/2$	$-5\kappa\eta$
δ	B_1+B_3	$a-b/2$	$\kappa(\gamma+\eta)$

In this paper, we assume that the form of the differential cross section is adequately described by Eq. (2) and discuss various experimental approaches to the measurement of β and the two nondipolar asymmetry parameters. We make specific use of Cooper's formulation [10], in which the nondipolar parameters are denoted by γ and δ and have been calculated for rare-gas subshells using a nonrelativistic central-potential model. Similar results have also been calculated by Bechler and Pratt [8], Amusia and Cherepkov [6], and Scofield [9], who used a relativistic central-potential model. Equivalent sets of parameters from alternative theoretical formulations [6,8,9] are compared with β, γ, and δ in Table I. Inclusion of two more asymmetry parameters makes the experimental measurement much more challenging than the single β parameter measurement. It is further complicated by the fact that commonly used synchrotron x rays are not completely linearly polarized. The purpose of this paper is to provide a road map for experimentalists by analyzing several experimental configurations and deriving formulations for the three parameters when partially linearly polarized x-ray beams are used. The requirement on the pointing accuracy of the photoelectron spectrometer is also discussed.

II. FORMULA FOR THE ANGULAR DISTRIBUTION

Cooper's formulation for the differential photoionization cross section using x rays linearly polarized along the z axis and propagating along the x axis is [10]

$$\left(\frac{d\sigma_{nl}}{d\Omega}\right)_z=\frac{\sigma_{nl}}{4\pi}\left[1+\frac{\beta}{2}\,(3\cos^2\theta-1)+(\delta+\gamma\cos^2\theta)\sin\theta\cos\phi\right]. \tag{3}$$

Here, β is the usual dipolar asymmetry parameter and δ and γ are additional parameters that characterize the forward-

backward asymmetry. Theoretical expressions for δ and γ involve radial dipole and quadrupole matrix elements and continuum-wave phase shifts [10]. As shown in Fig. 1, θ is the polar angle of the photoelectron momentum vector $\mathbf{p}$ with respect to the z axis or the photon polarization vector $\boldsymbol{\varepsilon}$, and ϕ is the azimuthal angle defined by the projection of $\mathbf{p}$ in the x-y plane, which is perpendicular to $\boldsymbol{\varepsilon}$ and contains the photon propagation vector $\mathbf{k}$. Note that Eq. (3) can be derived from Eq. (2) by the substitutions $|\boldsymbol{\varepsilon}\cdot\hat{\mathbf{p}}|\rightarrow\cos\theta$, $\hat{\mathbf{p}}\cdot\mathbf{k}\rightarrow\sin\theta\cos\phi$, $a\rightarrow\delta+\gamma/3$, and $b\rightarrow 2\gamma/3$.

Equation (3) shows that the nondipolar terms are maximal in the forward ($\phi=0°$) and backward ($\phi=180°$) directions with respect to $\mathbf{k}$ and vanish in the plane perpendicular to $\mathbf{k}$. That is, measurements in the plane perpendicular to $\mathbf{k}$ depend only on the dipolar asymmetry parameter β. Furthermore, measurements made in the plane perpendicular to $\mathbf{k}$ and with θ at the dipolar magic angle, $\theta=\cos^{-1}(1/\sqrt{3})\approx 54.7°$, are proportional to the angle-integrated cross section σ_{nl}, since the terms involving the asymmetry parameters vanish. Equation (3) also shows that the contribution of the δ parameter is proportional to $\sin\theta\cos\phi$, which is the x coordinate (or coordinate along $\mathbf{k}$) of the unit vector along $\mathbf{p}$. The contribution of the γ parameter is more complicated, depending in addition on a factor of $\cos^2\theta$.

For the case when the polarization vector $\boldsymbol{\varepsilon}$ is along the y axis, the angular distribution can be derived from Eq. (3) by a 90° rotation of the coordinate system about the x axis. We have

$$\left(\frac{d\sigma_{nl}}{d\Omega}\right)_y=\frac{\sigma_{nl}}{4\pi}\left[1+\frac{\beta}{2}(3\sin^2\theta\,\sin^2\phi-1)+(\delta+\gamma\sin^2\theta\,\sin^2\phi)\sin\theta\,\cos\phi\right]. \quad (4)$$

The angular distributions for unpolarized and circularly polarized x rays are the same [5] and can be derived by averaging Eqs. (3) and (4):

$$\left(\frac{d\sigma_{nl}}{d\Omega}\right)_{\text{unpol}}=\frac{\sigma_{nl}}{4\pi}\left[\left(1+\frac{\beta}{4}\right)+\left(\delta+\frac{\gamma}{2}\right)\sin\theta\,\cos\phi-\frac{3\beta}{4}\sin^2\theta\,\cos^2\phi-\frac{\gamma}{2}\sin^3\theta\,\cos^3\phi\right]. \quad (5)$$

Notice that Eq. (5) is a function only of $\sin\theta\cos\phi=\hat{\mathbf{p}}\cdot\hat{\mathbf{k}}$, the cosine of the angle between the electron momentum and photon propagation vectors.

III. ANGULAR DISTRIBUTION BY PARTIALLY LINEARLY POLARIZED X RAYS

X rays from a synchrotron radiation source are not only linearly polarized in the plane of the ring but also elliptically polarized outside this plane. To measure the dipolar and nondipolar parameters, the general expression for the photoelectron angular distribution by partially linearly polarized x rays has to be used.

It has been shown [16] that the photoelectron angular distribution corresponding to elliptically polarized light is the same as that produced by two perpendicular, incoherent, linearly polarized components aligned with the major and minor axes of the polarization ellipse. Let I_{major} and I_{minor} denote the intensities of the components along major and minor axes, respectively. The elliptically polarized light can now be treated as a linearly polarized component with intensity

$$I_{\text{pol}}=I_{\text{major}}-I_{\text{minor}},$$

and an unpolarized component with the rest of the total intensity.

The degree of linear polarization P can be defined as the ratio of linearly polarized intensity to the total x-ray intensity

$$P\equiv\frac{I_{\text{pol}}}{I_{\text{total}}},$$

where I_{total} is the total intensity of the x rays. For elliptically polarized x rays, we have

$$P=\frac{I_{\text{major}}-I_{\text{minor}}}{I_{\text{total}}}.$$

It follows that $0\leqslant P\leqslant 1$, and having $P=1$ represents completely linearly polarized x rays, while having $P=0$ corresponds to unpolarized or circularly polarized x rays.

If we choose the coordinate system such that the z axis aligns with the major axis of the polarization ellipse as shown in Fig. 1, the photoelectron angular distribution can be expressed as

$$\frac{d\sigma_{nl}}{d\Omega}(P)=\frac{I_{\text{pol}}}{I_{\text{total}}}\left(\frac{d\sigma_{nl}}{d\Omega}\right)_z+\frac{I_{\text{total}}-I_{\text{pol}}}{I_{\text{total}}}\left(\frac{d\sigma_{nl}}{d\Omega}\right)_{\text{unpol}},$$

or

$$\frac{d\sigma_{nl}}{d\Omega}(P)=P\left(\frac{d\sigma_{nl}}{d\Omega}\right)_z+(1-P)\left(\frac{d\sigma_{nl}}{d\Omega}\right)_{\text{unpol}}.$$

By using Eqs. (3) and (5), we derive [17]

$$\frac{d\sigma_{nl}}{d\Omega}(P)=\frac{\sigma_{nl}}{4\pi}\left\{\left[1+\frac{\beta}{4}-\frac{3}{4}P\beta+\frac{3}{2}P\beta\,\cos^2\theta\right]+\left[\delta+\gamma P\,\cos^2\theta-\gamma\,\frac{(P-1)}{2}\right]\sin\theta\,\cos\phi+\left[\frac{3\beta}{4}(P-1)\right]\sin^2\theta\,\cos^2\phi+\left[\gamma\,\frac{(P-1)}{2}\right]\sin^3\theta\,\cos^3\phi\right\}.$$

With replacement of $\cos^2\phi$ and $\cos^3\phi$ with equivalent expressions using $\cos 2\phi$ and $\cos 3\phi$, the angular distribution becomes

$$\frac{d\sigma_{nl}}{d\Omega}(P) = \frac{\sigma_{nl}}{4\pi}\left\{\left[1+\frac{\beta}{8}(1+3P)(3\cos^2\theta-1)\right] + \left[\delta+\gamma\cos^2\theta+\gamma\frac{(P-1)}{8}(5\cos^2\theta-1)\right]\times\sin\theta\cos\phi+\left[\frac{3\beta}{8}(P-1)\right]\sin^2\theta\cos2\phi + \left[\gamma\frac{(P-1)}{8}\right]\sin^3\theta\cos3\phi\right\}. \quad (6)$$

It should be pointed out that the same expression as Eq. (6) can be derived directly from Eqs. (3) and (4) without using Eq. (5). However, the above derivation also demonstrates the case of x rays with circularly polarized components as is the case of synchrotron x rays when not aligned with the plane of the ring.

In practice, there may be a tilt between the experimentally defined coordinate axes and the linear polarization component. This situation is represented in Fig. 2, where the linear component lies in the y-z plane but at a tilt angle ψ with respect to the z axis. The experimentally observed angular distribution is then given by a rotation of the coordinate system by an angle ψ about the x axis:

$$\frac{d\sigma_{nl}}{d\Omega}(P,\psi) = \frac{\sigma_{nl}}{4\pi}\left\{\left[1+\frac{\beta}{8}(1+3P\cos2\psi)(3\cos^2\theta-1)\right] + \left[\delta+\gamma\cos^2\theta+\frac{\gamma}{8}(P\cos2\psi-1)\times(5\cos^2\theta-1)\right]\sin\theta\cos\phi + \left[\frac{3\beta}{8}(P\cos2\psi-1)\right]\sin^2\theta\cos2\phi + \left[\frac{\gamma}{8}(P\cos2\psi-1)\right]\sin^3\theta\cos3\phi - \left[\frac{3\beta}{2}(P\sin2\psi\cos\theta)\right]\sin\theta\sin\phi - \left[\frac{\gamma}{2}(P\sin2\psi\cos\theta)\right]\sin^2\theta\sin2\phi\right\}. \quad (7)$$

Note that when $\psi=90°$, the above expression corresponds to the case when the linear-polarization component lies along the y axis.

Equation (7) is in the form of the Fourier expansion of the angular distribution in terms of the ϕ angle, if the θ angle is fixed. When θ is at the magic angle of 54.7°, the constant term is proportional to the angle-integrated cross section σ_{nl}, as in the case of dipole approximation.

We shall use Eqs. (6) and (7) to analyze several experimental configurations and formulate the dipolar and nondipolar parameters for partially linearly polarized x rays. The effects resulting from possible mechanical misalignment in the experiments will also be discussed, to help in designing such experiments.

IV. ANALYSIS OF EXPERIMENTAL CONFIGURATIONS

Angle-resolved electron-energy analyzers (EEA) are commonly used for measuring the angular distribution of photoelectrons excited from a specific atomic subshell. The angular distribution can be measured either by placing several fixed EEA's around the sample or by placing one EEA on a rotational device [15].

If the fixed or rotating EEA's are arranged to measure electrons with momentum vectors at a fixed polar angle θ, then the measured data as a function of azimuthal angle ϕ will be the Fourier series expressed in Eq. (7). The Fourier coefficients can be extracted by numerical Fourier series expansion, and the values of the dipolar and nondipolar coefficients can be deduced. We consider several experimental configurations in the following discussion.

A. Polarization vector along the z axis

1. θ fixed at an arbitrary angle

Equation (6) describes the angular distribution of a ϕ scan at fixed θ with the linear polarization vector pointing along the z axis as shown in Fig. 3. Here, the EEA is rotating about the photon polarization vector $\boldsymbol{\varepsilon}$ or the z axis and measuring photoelectrons with momentum vector $\mathbf{p}$, which are at a fixed angle θ with respect to the z axis. For a single ϕ scan, the measured data can be fitted to a function of the form

$$a_0[1+a_1\cos\phi+a_2\cos2\phi+a_3\cos3\phi],$$

and four coefficients can be obtained (a_0, a_1, a_2, and a_3). With these coefficients, we can yield four equations for five variables (σ_{nl}, β, δ, γ, and P) from Eq. (6). In principle, if one variable is known, all others can be solved. However, for an experiment with highly polarized synchrotron light, a_2

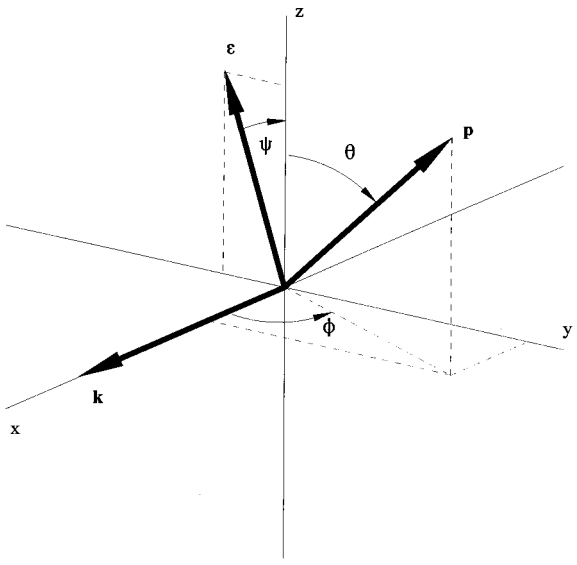

FIG. 2. The coordinate system with the major polarization vector in the y-z plane and tilted at angle ψ with respect to the z axis.

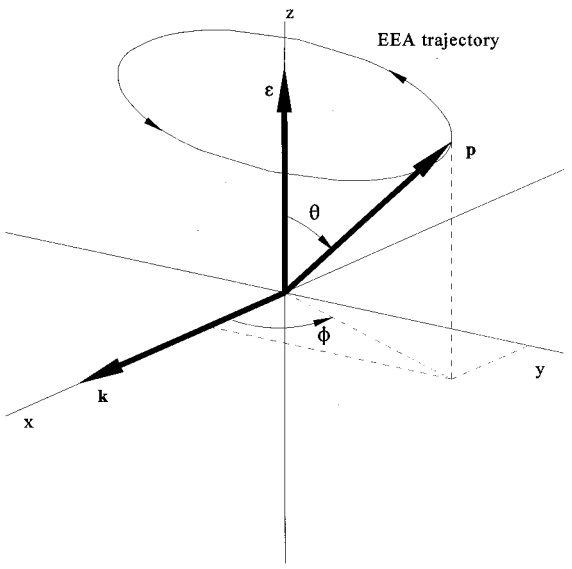

FIG. 3. The coordinate system with the major polarization vector along the z axis. The trajectory for a ϕ scan with fixed θ by the EEA is also shown.

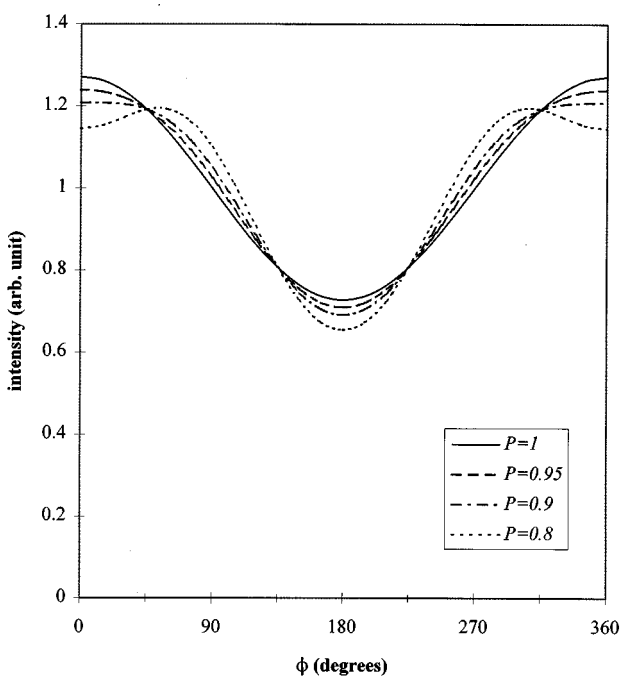

FIG. 4. Photoelectron angular distribution as a function of ϕ, with θ at magic angle and $\beta=2$, $\gamma=1$, and $\delta=0$. The four curves, corresponding to $P=1$, $P=0.95$, $P=0.9$, and $P=0.8$, are shown.

and a_3 are small because they vary as $P-1$, and the solution for the variables, despite the complex mathematical expression, could have large error bars. A simpler configuration with θ fixed at the magic angle is discussed below.

2. θ fixed at the magic angle

With θ fixed at the magic angle of 54.7°, as was done in Ref. [15], the constant term in the Fourier series of Eq. (6) becomes unity, and independent of β and P. Equation (6) becomes

$$\frac{d\sigma_{nl}}{d\Omega}(P)=\frac{\sigma_{nl}}{4\pi}\left\{1+\left[\delta+\gamma\frac{(P+3)}{12}\right]\sqrt{\frac{2}{3}}\cos\phi+\beta\frac{(P-1)}{4}\cos2\phi+\gamma\frac{(P-1)}{12}\sqrt{\frac{2}{3}}\cos3\phi\right\}.$$

As stated in Sec. IV A 1, the coefficients of the $\cos2\phi$ and $\cos3\phi$ terms of the above expression are usually small for highly polarized synchrotron x rays (i.e., P is close to 1), and they cannot be used directly to precisely calculate β or γ. From the coefficients of the $\cos\phi$ and $\cos3\phi$ terms, we have

$$\delta+\frac{\gamma}{3}=\sqrt{\tfrac{3}{2}}(a_1-a_3).$$

Although δ and γ parameters cannot be separated accurately for highly polarized x rays in this configuration, a weighted sum of δ and γ can be determined, independent of the polarization P, and compared to theoretical values [15]. Figure 4 shows the photoelectron intensity as a function of ϕ for several P values for $\beta=2$, $\delta=0$, and $\gamma=1$. Notice that when ϕ is 45°, 135°, 225°, or 315°, the intensities depend only on a_1-a_3 and, therefore, are independent of P. This result is an example of a general symmetry property of angular distributions by which the dependence on the polarization state of the photon beam can be eliminated [5].

This configuration is most useful in cases where $\delta=0$ (i.e., excitation from s subshells in a nonrelativistic central potential model [10]) and the above equation becomes

$$\gamma=\sqrt{\tfrac{27}{2}}(a_1-a_3).$$

Furthermore, for $\delta=0$, the degree of polarization P can be calculated using

$$P=\frac{a_1+3a_3}{a_1-a_3},$$

provided that γ, or a_1-a_3, is large enough to yield P with good accuracy. We can also calculate P by using

$$P=\frac{4}{\beta}a_2+1.$$

This expression is useful when β is known from other measurements or calculations, or when it is valid to assume $\beta\approx2$ for an s subshell.

The a_0 coefficient in the Fourier series is proportional to the angle-integrated cross section, σ_{nl}. The x-ray energy dependence of σ_{nl} can be measured by scanning the x-ray energy.

B. Polarization vector along the *y* axis

1. θ fixed at an arbitrary angle

When the polarization vector is along the y axis, as shown in Fig. 5, the EEA's rotation axis, the z axis, is perpendicular to the photon polarization vector $\boldsymbol{\varepsilon}$, or the y axis, and the EEA is measuring photoelectrons with momentum vector **p**,

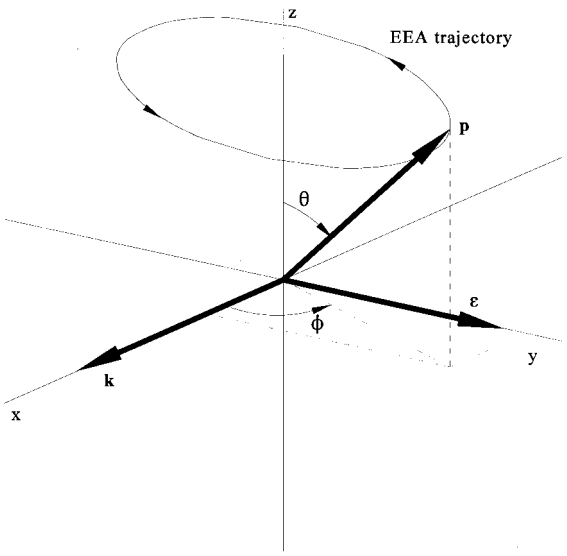

FIG. 5. Same as Fig. 3, but with the major polarization vector along the y axis.

which are at a fixed angle θ with respect to the EEA's axis of rotation. The angular distribution can be derived by letting $\psi=90°$ in Eq. (7), to give

$$\frac{d\sigma_{nl}}{d\Omega}\left(P,\psi=\frac{\pi}{2}\right)=\frac{\sigma_{nl}}{4\pi}\left\{\left[1+\frac{\beta}{8}(1-3P)(3\cos^2\theta-1)\right]+\left[\delta+\gamma\cos^2\theta-\gamma\frac{(P+1)}{8}\times(5\cos^2\theta-1)\right]\sin\theta\cos\phi-\left[\frac{3\beta}{8}(P+1)\right]\sin^2\theta\cos2\phi-\left[\gamma\frac{(P+1)}{8}\right]\sin^3\theta\cos3\phi\right\}.$$

Unlike the previous configuration discussed in Sec. IV A, the Fourier coefficients do not approach zero with highly linearly polarized light (i.e., $P\approx1$). By fitting the data of a single ϕ scan, we have again four equations and five variables (σ_{nl}, β, δ, γ, and P). By knowing any one variable, the other variables can be solved, although the general expression for the solution can be quite complex. However, we note that the ratio of γ and β can be simply expressed by

$$\frac{\gamma}{\beta}=\frac{3}{\sin\theta}\frac{a_3}{a_2},$$

where a_2 and a_3 are the experimentally best-fitted Fourier coefficients discussed previously.

2. θ fixed at the magic angle

When θ is set to the magic angle, the angular distribution becomes

$$\frac{d\sigma_{nl}}{d\Omega}(P)=\frac{\sigma_{nl}}{4\pi}\left\{1+\left[\delta+\gamma\frac{(-P+3)}{12}\right]\sqrt{\frac{2}{3}}\cos\phi-\beta\frac{(P+1)}{4}\cos2\phi-\gamma\frac{(P+1)}{12}\sqrt{\frac{2}{3}}\cos3\phi\right\}.$$

Again, none of the Fourier coefficients become insignificant when P is close to 1. With the experimentally best-fitted Fourier coefficients of a_1, a_2, and a_3, we have

$$\beta=-\frac{4}{(1+P)}a_2,$$

$$\gamma=-12\sqrt{\frac{3}{2}}\frac{1}{(1+P)}a_3,$$

and

$$\delta=\sqrt{\frac{3}{2}}\left(a_1+\frac{3-P}{1+P}a_3\right).$$

If the value of P is known, all β, δ, and γ parameters can be determined by a single ϕ scan. In addition, the energy dependence of the total cross section σ_{nl}, can be determined by the Fourier coefficient, a_0. One can determine P from these equations if either δ or β is known. For example, in the limit of a nonrelativistic central field model [10], theory shows that $\delta=0$ and $\beta=2$ for s subshells. Once P is determined by s-subshell electrons or other independent techniques, the β, δ, and γ parameters for all other subshells can be measured by using the equations above.

For highly polarized synchrotron x rays, we can define $\Delta P\equiv1-P$, and the expressions for β and γ parameters can be approximated for small ΔP by

$$\beta\approx-2\left(1+\frac{\Delta P}{2}\right)a_2,$$

$$\gamma\approx-6\sqrt{\frac{3}{2}}\left(1+\frac{\Delta P}{2}\right)a_3,$$

and

$$\delta=\sqrt{\frac{3}{2}}(a_1+a_3)-\frac{\gamma}{6}\Delta P.$$

The above equations show that, for a 90% linearly polarized x-ray beam, there will only be 5% change in the values of β and γ from those for a completely linearly polarized x-ray beam. Also, for a value of γ around unity [10], the change in the value of δ is about 0.02. Judging from the theoretical values of Ref. [10], the influence of partial polarization from a synchrotron x-ray beam on the measurement of the β and γ parameters is quite small in most cases. However, it can be quite significant for the δ parameter.

3. θ fixed at angle 90°

An interesting case to consider is when the polar angle $\theta=90°$ and the linearly polarized component of the x-ray beam lie along the y axis. In this case, the EEA is rotating in

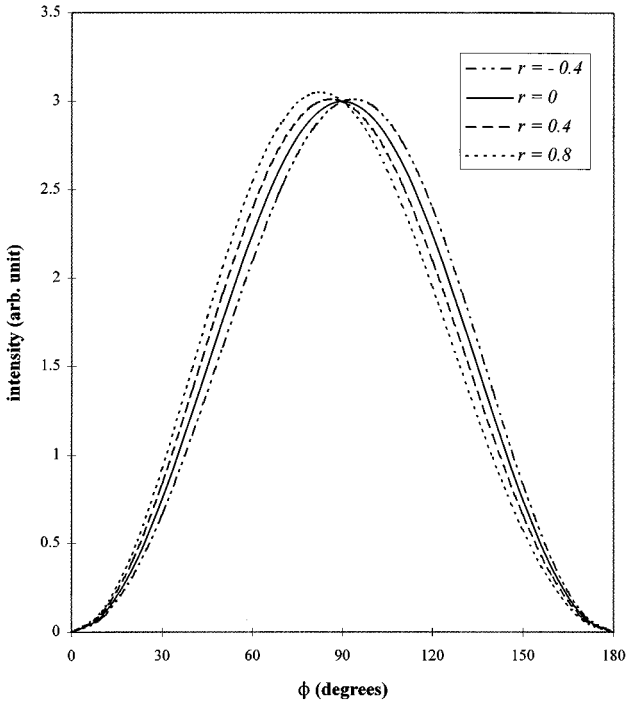

FIG. 6. Angular distribution, as a function of ϕ, in the plane containing both the photon propagation vector **k** and the polarization vector $\boldsymbol{\varepsilon}$ for $\gamma=-0.4$, $\gamma=0$, $\gamma=0.4$, and $\gamma=0.8$, and assuming $\beta=2$ and $\delta=0$.

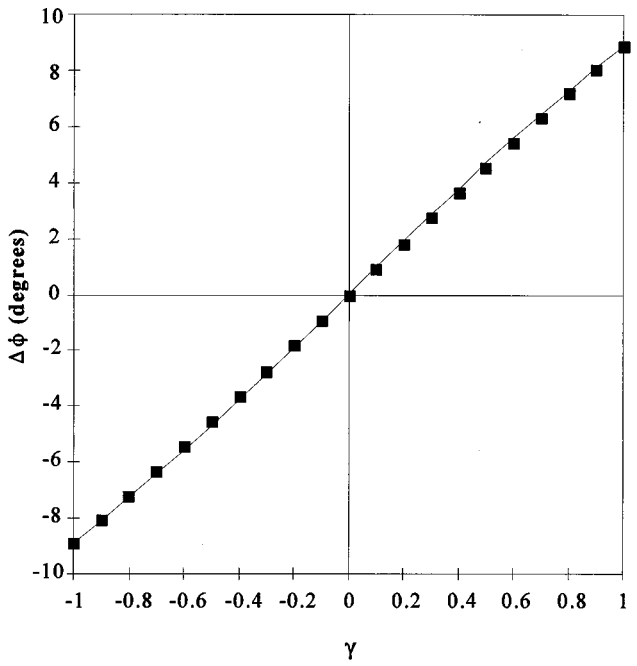

FIG. 7. The phase shift angle $\Delta\phi$ as a function of γ, for $\beta=2$ and $\delta=0$. The solid line is the actual $\Delta\phi$, and the squares are the best-fit $\Delta\phi$. The functional form used to fit the calculated angular distribution is $\sin^2(\phi+\Delta\phi)$. The total range of ϕ for the fit is 40°, centered at $\phi=90°$.

the x-y plane, which contains the photon momentum vector and the polarization vector. The angular distribution is expressed from Eq. (7), with $\psi=90°$ and $\theta=90°$, as follows:

$$\frac{d\sigma_{nl}}{d\Omega}(P)=\frac{\sigma_{nl}}{4\pi}\left\{\left[1-\frac{\beta}{8}(1-3P)\right]+\left[\delta+\frac{\gamma}{8}(P+1)\right]\cos\phi-\left[\frac{3\beta}{8}(P+1)\right]\cos2\phi-\left[\frac{\gamma}{8}(P+1)\right]\cos3\phi\right\}. \tag{8}$$

The constant term is dependent on both β and P. Furthermore, the actual range of ϕ that can be measured is limited by the physical size of the EEA, because it can block the incident x rays, and a limited ϕ scan reduces the accuracy of the Fourier-series fit. A better method follows from Fig. 6, which shows the angular distribution for several values of γ, with $\delta=0$ and $\beta=2$. The angular distribution for $\gamma=0$ (i.e., the dipole approximation) in Fig. 6 is given by

$$\frac{d\sigma_{nl}}{d\Omega}(P)=\frac{\sigma_{nl}}{4\pi}\frac{3(P+1)}{2}\sin^2\phi,$$

which has a $\sin^2\phi$ dependency and maximum intensity for $\phi=90°$. As the value of γ is increased, the angle ϕ that corresponds to the maximum intensity gradually shifts away from the angle $\phi=90°$. This is true because the γ parameter is mainly responsible for the forward-backward asymmetry that deviates from the angular distribution given by the dipole approximation. Mathematically, we can calculate the angle $\phi_{\max}$ that corresponds to the maximum intensity of Eq. (8) by setting its derivative with respect to ϕ to zero. The result is

$$\frac{\gamma}{\beta}=\frac{3\cos\phi_{\max}}{1-3\cos^2\phi_{\max}},$$

if we assume $\delta=0$. Notice that the ratio γ/β depends only on $\phi_{\max}$ and is independent of P. Furthermore, we can define the phase shift $\Delta\phi$ as

$$\Delta\phi\equiv\frac{\pi}{2}-\phi_{\max}.$$

For a small $\Delta\phi$, the γ parameter can be approximated by

$$\gamma\approx\beta(3\Delta\phi+\tfrac{17}{2}\Delta\phi^3),$$

or, when we have $\beta=2$, $\gamma\approx6\Delta\phi+17\Delta\phi^3$.

A method to determine the phase shift $\Delta\phi$ in experimental work is to measure a section of the angular distribution around $\phi=90°$, and the measured data can be fitted with the function $\sin^2(\phi+\Delta\phi)$. The γ parameter follows directly from the best-fit $\Delta\phi$ value. The result of a simulation of this method is shown in Fig. 7, where we plot $\Delta\phi$ as a function of γ with $\delta=0$ and $\beta=2$. The square dots in Fig. 7 represent values of $\Delta\phi$ obtained by fitting the theoretical angular distribution with the function $\sin^2(\phi+\Delta\phi)$ over a total range of ϕ of 40°, centered at 90°.

Although limited to s-subshell electrons, this method does not require a large angle of rotation by the EEA. Rotation in the x-y plane also reduces the mechanical complexity of

setting the magic angle as in previous cases. This method is again independent of the polarization P of the x-ray beam.

V. EFFECTS OF THE ROTATION AXIS TILT

In this section, we discuss the effects of misalignment of the EEA rotation axis with the polarization and propagation axes of the x-ray beam. The sources of this error can be the mechanical uncertainty in positioning the EEA and the uncertainty in determining the direction of the polarization vector. We can discuss the tilt angle of the EEA rotational-axis misalignment in two directions, one in the y-z plane and the other in the x-z plane.

A. Tilt in the y-z plane

When the major polarization vector is along the z axis, as shown in Fig. 3 and discussed in Sec. IV A, the angular distribution is expressed in Eq. (6). By tilting the rotation axis in the y-z plane by an angle ψ the geometry is as shown in Fig. 2 and the observed angular distribution becomes Eq. (7). Comparing Eqs. (6) and (7), we can observe two differences. First, for $\psi \neq 0$, two more terms appear in the Fourier expansion, the $\sin\phi$ and the $\sin(2\phi)$ terms. Both terms have a linear dependency on ψ, when ψ is small, and they can be identified from the Fourier expansion of the ϕ-scan data. Second, for the other Fourier expansion terms, the polarization P is replaced by $P\cos(2\psi)$. It follows that the derivations discussed in Sec. IV A 2 remain unchanged, even for $\psi \neq 0$, with the exception that the ''effective'' value of P is now multiplied by a factor of $\cos(2\psi)$. The tilt in the y-z plane bears no influence on the determination of the γ parameter.

A similar argument can be applied to the case where the major polarization vector is along the y axis, as discussed in Sec. IV B. The expressions in Sec. IV B 2 of the β, γ, and δ parameters are not affected by the tilt angle, except that the polarization P in these expressions is replaced by $P\cos(2\psi)$. In addition, the magnitude of the $\sin\phi$ and $\sin(2\phi)$ terms in the Fourier series can be used to estimate the tilt angle ψ, even though the precise orientation of the polarization vector in the y-z plane is not crucial for determining the dipolar and nondipolar parameters.

B. Tilt in the x-z plane

For a tilt in the x-z plane, the axis of rotation of the EEA leans forward or backward with respect to the photon propagation direction. The general expression for the angular distribution can be derived from Eq. (6) by a rotation of the coordinate system about the y axis. The result is much more complex, and we give only the first-order approximation for a small tilt angle η:

$$\begin{aligned}\frac{d\sigma_{nl}}{d\Omega}(P,\eta) = \frac{\sigma_{nl}}{4\pi}\Bigg\{&\left[1+\frac{\beta}{8}(1+3P)(3\cos^2\theta-1)\right]\\&+\left[\delta+\frac{\gamma}{4}(2+2P-(3+5P)\sin^2\theta)\right]\cos\theta\,\eta\\&+\Bigg[\delta+\gamma\cos^2\theta+\gamma\frac{(P-1)}{8}(5\cos^2\theta-1)\\&-\frac{3\beta}{2}(3P-1)\cos\theta\,\eta\Bigg]\sin\theta\cos\phi\\&+\Bigg[\frac{3\beta}{8}(P-1)-\frac{\gamma}{4}(P+3)\\&\times\cos\theta\,\eta\Bigg]\sin^2\theta\cos2\phi\\&+\left[\gamma\frac{(P-1)}{8}\right]\sin^3\theta\cos3\phi\Bigg\}. \qquad (9)\end{aligned}$$

Unlike a tilt in the y-z plane, a tilt in the x-z plane does not generate new terms in the Fourier expansion, and the tilt cannot be identified easily from the Fourier analysis of the data. Comparing Eq. (9) with Eq. (6), we can see that the perturbation introduced by the tilt angle η on the $\cos\phi$ and $\cos(2\phi)$ terms of the Fourier series is substantial. We can understand this effect by noting that the nondipolar parameters result in the bending of the dipole angular distribution forward or backward with respect to the photon propagation direction. A tilt by the rotation axis of the EEA in the same sense will change the measured asymmetry properties, and therefore the calculated values, of the nondipolar parameters.

To quantify the effect of a tilt in the x-z plane, we set the θ angle in Eq. (9) at the magic angle and examine the results of Sec. IV A 2 depicted by Fig. 3. For the case when $\delta=0$, we have, from Eq. (9),

$$\begin{aligned}\frac{d\sigma_{nl}}{d\Omega}(P,\eta) = \frac{\sigma_{nl}}{4\pi}\Bigg\{&\left[1-\frac{\gamma P}{3\sqrt{3}}\,\eta\right]+\Bigg[\gamma\frac{(P+3)}{12}\sqrt{\frac{2}{3}}\\&-\frac{1}{\sqrt{2}}\beta(3P-1)\,\eta\Bigg]\cos\phi\\&+\left[\frac{\beta}{4}(P-1)-\frac{\gamma}{6\sqrt{3}}(P+3)\,\eta\right]\cos2\phi\\&+\left[\gamma\frac{(P-1)}{12}\sqrt{\frac{2}{3}}\right]\cos3\phi\Bigg\}.\end{aligned}$$

The constant term in the above equation now includes unity and a correction term dependent on γ, P, and η. This correction term is typically smaller than 0.01 for a tilt angle η of about 1° and γ around unity [10], so it is usually negligible.

Following Sec. IV A 2, the expression for γ now becomes

$$\gamma = 3\sqrt{\frac{3}{2}}(a_1-a_3)+\frac{3\sqrt{3}}{2}\beta(3P-1)\,\eta.$$

The second term determines the uncertainty in measuring γ from an unknown tilt angle η. For $\beta=2$ and $P\approx1$, the last term is approximately 10η. This result indicates that, if the rotation axis of the EEA has a pointing accuracy of 1° in the x-z plane, the uncertainty in measuring γ is 0.17, which is quite a significant error, considering that the theoretical values for γ are usually less than 1 in the soft-x-ray range [10].

For the case where the major polarization vector is along the y axis, as discussed in Sec. IV B 2 and depicted in Fig. 5,

the approximate angular distribution for a small tilt angle η, when θ is at the magic angle, is given by

$$\frac{d\sigma_{nl}}{d\Omega}(P,\eta)=\frac{\sigma_{nl}}{4\pi}\left\{\left[1+\frac{1}{\sqrt{3}}\left(\delta+\frac{\gamma P}{3}\right)\eta\right]\right.$$
$$+\left[\left(\delta+\gamma\frac{(-P+3)}{12}\right)\sqrt{\frac{2}{3}}\right.$$
$$\left.+\frac{1}{\sqrt{2}}\beta(3P+1)\eta\right]\cos\phi-\left[\frac{\beta}{4}(P+1)\right.$$
$$\left.+\frac{\gamma}{6\sqrt{3}}(-P+3)\eta\right]\cos2\phi$$
$$\left.-\left[\gamma\frac{(P+1)}{12}\sqrt{\frac{2}{3}}\right]\cos3\phi\right\}.$$

As discussed in Sec. IV B 2, the advantage of this configuration is that none of the Fourier coefficients approach zero with the high degree of polarization of the x-ray beam. To simplify the above equation, we first note that the constant term in the Fourier expansion has a first-order term in η. This term is typically smaller than 1% and can be ignored. With highly polarized x rays ($P\approx1$), we can further approximate the above equation by

$$\frac{d\sigma_{nl}}{d\Omega}(P,\eta)=\frac{\sigma_{nl}}{4\pi}\left\{1+\left[\left(\delta+\gamma\frac{(-P+3)}{12}\right)\sqrt{\frac{2}{3}}\right.\right.$$
$$\left.+\frac{4}{\sqrt{2}}\beta\eta\right]\cos\phi-\left[\frac{\beta}{4}(P+1)\right.$$
$$\left.\left.+\frac{\gamma}{3\sqrt{3}}\eta\right]\cos2\phi-\left[\gamma\frac{(P+1)}{12}\sqrt{\frac{2}{3}}\right]\cos3\phi\right\}.$$

Following the same derivation as in Sec. IV B 2, we obtain

$$\beta=-2\left(1+\frac{\Delta P}{2}\right)a_2-\frac{2}{3\sqrt{3}}\gamma\eta,$$

$$\gamma=-6\sqrt{\frac{3}{2}}\left(1+\frac{\Delta P}{2}\right)a_3,$$

and

$$\delta=\sqrt{\frac{3}{2}}(a_1+a_3)-\frac{\gamma}{6}\Delta P-2\sqrt{3}\beta\eta.$$

The above expressions show that the γ parameter is not affected by the tilt angle η, but substantial error could occur for the β and δ parameters if the tilt angle were not taken into consideration. For example, if we have $\beta=1$ and $\gamma=1$, and the rotation axis of the EEA has a pointing accuracy of 1° in the x-z plane, then the uncertainty in the β and δ parameters would be 0.007 and 0.06, respectively. The δ parameter is roughly an order of magnitude more sensitive to the pointing error of the rotation axis of the EEA in the x-z plane than is the β parameter.

One method for determining the tilt angle η experimentally is by making a ϕ scan for s-subshell photoelectrons, where we can assume $\beta=2$ and $\delta=0$. Both η and ΔP can then be calculated from the Fourier parameters a_1, a_2, and a_3, by solving the linear equations

$$\sqrt{2}a_3\eta-\frac{a_2}{2}\Delta P=(1+a_2)$$

$$4\sqrt{2}\eta-a_3\Delta P=(a_1+a_3).$$

Once η and ΔP are determined, the dipolar and nondipolar parameters for any other subshells can be measured.

The results of this section indicate that tilt errors in the x-z plane are more problematic, for the measurement of asymmetry parameters, than are tilt errors in the y-z plane. For the configuration described in Sec. IV A 2, a high pointing accuracy for the rotation axis of the EEA is required. Fortunately, it is feasible to precisely position the rotation axis of an EEA perpendicular to the propagation direction of the x-ray beam by the use of mechanical and optical alignment methods [15]. On the other hand, for the configuration described in Sec. IV B 2 the tilt angle can first be measured by using s-subshell electrons, and then the tilt angle and the polarization can be used for other subshells.

VI. CONCLUSIONS

We described several experimental approaches for extracting the dipolar and nondipolar parameters, β, γ, and δ, using partially polarized light and Fourier-series data analysis. When the EEA is rotating about the direction of the polarization vector, the expression for angular distribution can be simplified with the angle θ between the polarization vector and the photoelectron momentum vector fixed at the magic angle. Measurement from this geometry can yield, independent of the degree of polarization, a linear combination of γ and δ, whereas β cannot be determined for highly polarized x rays. This geometry is most useful in measuring the γ parameter for s-subshell electrons. When the EEA is rotating about an axis perpendicular to both the polarization vector and the photon propagation vector, all β, γ, and δ parameters can be determined, provided that the degree of polarization of the x-ray beam is known. In addition, the degree of polarization of the x-ray beam can be determined by this geometry using s-subshell electrons. The mathematical expressions for the β, γ, and δ parameters were given for θ fixed at the magic angle. A much simpler configuration was discussed where the EEA is rotating in the plane containing the photon momentum vector and the photon propagation vector. In this case, the ratio of γ and β is a function of the phase shift of the angular distribution, when $\delta=0$, and is independent of the degree of polarization of the x-ray

beam. When used to measure s-subshell electrons, the γ parameter can be determined. Finally, we showed that the pointing precision of the rotation axis of the EEA is critical in the forward-backward direction. These approaches can be used in experiments, so that the breakdown of the dipole approximation can be measured and compared with theory.

ACKNOWLEDGMENTS

The authors would like to thank Dr. R. D. Deslattes for inspiring discussions. U.A. is very grateful to the Alexander von Humboldt Foundation for support within the Feodor Lynen Program.

[1] S. T. Manson and D. Dill, in *Electron Spectroscopy: Theory, Techniques, and Applications*, edited by C. R. Brundle and A. D. Baker (Academic, New York, 1978), Vol. 2, pp. 157–195.

[2] A. F. Starace, in *Theory of Atomic Photoeffect*, edited by W. Mehlhorn, *Handbuch der Physik*, Vol. XXXI (Springer-Verlag, Berlin, 1982), pp. 1–121.

[3] M. Ya. Amusia, *Atomic Photoeffect* (Plenum, New York, 1990).

[4] V. Schmidt, Rep. Prog. Phys. **55**, 1483 (1992).

[5] M. Peshkin, Adv. Chem. Phys. **18**, 1 (1970); and unpublished.

[6] M. Ya. Amusia and N. A. Cherepkov, *Case Studies in Atomic Physics* (North-Holland, Amsterdam, 1975), Vol. 5, pp. 47–179.

[7] A. Ron, R. H. Pratt, and H. K. Tseng, Chem. Phys. Lett. **47**, 377 (1977); H. K. Tseng, R. H. Pratt, S. Yu, and A. Ron, Phys. Rev. A **17**, 1061 (1978).

[8] A. Bechler and R. H. Pratt, Phys. Rev. A **39**, 1774 (1989); **42**, 6400 (1990).

[9] J. H. Scofield, Phys. Rev. A **40**, 3054 (1989); Phys. Scr. **41**, 59 (1990).

[10] J. W. Cooper, Phys. Rev. A **47**, 1841 (1993).

[11] A. C. Parr, S. H. Southworth, J. L. Dehmer, and D. M. P. Holland, Nucl. Instrum. Methods **222**, 221 (1984).

[12] S. H. Southworth, C. M. Truesdale, P. H. Kobrin, D. W. Lindle, W. D. Brewer, and D. A. Shirley, J. Chem. Phys. **76**, 143 (1982).

[13] J. Feldhaus, W. Erlebach, A. L. D. Kilcoyne, K. J. Randall, and M. Schmidbauer, Rev. Sci. Instrum. **63**, 1454 (1992).

[14] M. O. Krause, Phys. Rev. **177**, 151 (1969); F. Wuilleumier and M. O. Krause, Phys. Rev. A **10**, 242 (1974).

[15] B. Krässig, M. Jung, D. S. Gemmell, E. P. Kanter, T. LeBrun, S. H. Southworth, and L. Young, Phys. Rev. Lett. **75**, 4736 (1995); M. Jung, B. Krässig, D. S. Gemmell, E. P. Kanter, T. LeBrun, S. H. Southworth, and L. Young (unpublished).

[16] J. A. R. Samson and A. F. Starace, J. Phys. B **8**, 1806 (1975); corrigendum, J. Phys. B **12**, 3993 (1979).

[17] The cross section for partially polarized x rays given in Eq. (24) of Ref. [10] is missing the term containing $\sin^2\theta\cos^2\phi$.